MIT Libraries | DSpace@MIT

MIT Open Access Articles

Effect of feed salinity on the performance of humidification dehumidification desalination

The MIT Faculty has made this article openly available. ***Please share*** how this access benefits you. Your story matters.

Citation: Chehayeb, Karim M., and John H. Lienhard V. "Effect of feed salinity on the performance of humidification dehumidification desalination." 2015 IDA World Congress on Desalination and Water Reuse (August 2015).

Publisher: International Desalination Association

Persistent URL: http://hdl.handle.net/1721.1/99722

Version: Author's final manuscript: final author's manuscript post peer review, without publisher's formatting or copy editing

Terms of use: Creative Commons Attribution-Noncommercial-Share Alike

Massachusetts Institute of Technology

EFFECT OF FEED SALINITY ON THE PERFORMANCE OF HUMIDIFICATION DEHUMIDIFICATION DESALINATION

Authors: ***Karim M. Chehayeb****, John H. Lienhard V*

Presenter: **Karim M. Chehayeb**
Doctoral Candidate – Massachusetts Institute of Technology – USA
chehayeb@mit.edu

Abstract

Humidification dehumidification (HDH) is a thermal desalination technology that imitates the rain cycle in an engineered setting. It can be advantageous is small-scale, decentralized applications. In addition, the components used in HDH systems are fairly robust, and can treat highly saline water. The technology has recently been commercialized in order to treat highly saline produced water from hydraulically fractured oil and gas wells. That plant has proved HDH's ability to treat water that most current seawater desalination technologies are unable to treat.

The major disadvantage of HDH is its low energy efficiency compared to other desalination technologies when treating seawater. Previous studies have shown that the system's energy efficiency can be improved greatly by varying the water-to-air mass flow rate ratio within the system. This translates into operating two or more adjacent stages at different mass flow rate ratios, which is done by extracting an air stream from an intermediate location in the humidifier and injecting it at an intermediate location in the dehumidifier.

Previous models have used fixed effectiveness or fixed pinch approaches to evaluate the benefits of multi-staging, but these do not take account of the size of the system. In physical systems, what remains constant when going from a single-stage to a multi-stage system is the total size of the system and not the effectiveness or the pinch. Therefore, comparing systems with the same total heat exchanger area is the best way to understand the effect of extraction/injection and whether its implementation is beneficial or not.

In this paper, a numerical heat and mass transfer model is used to simulate the operation of HDH at various feed salinities. For each case, the performance of the single-stage system is compared to that of a two-stage system of the same size at different values of feed salinity. The ability of HDH to treat feeds with varying salinity is also studied.

I. INTRODUCTION

Humidification dehumidification (HDH) is a thermal desalination technology that can be advantageous in small scale, decentralized applications [1, 2, 3]. The technology does not use membranes or hot metal surfaces, which allows it to treat highly saline water with some oil content. In addition, the equipment in HDH can be replaced cheaply if scaling does occur. These characteristics make HDH suitable for treating produced water from hydraulically fractured oil and gas wells. In fact, HDH has recently been commercialized, and was shown to treat very saline water from shale wells that most other technologies have so far failed to treat [4].

A typical humidification dehumidification (HDH) system consists of a humidifier, a dehumidifier, and a heater. As shown in Fig. 1, cold air is put in direct contact with a stream of hot saline water in the humidifier, causing the air to heat up and carry more water vapor. The hot moist air is then put in indirect contact with cold saline water in the dehumidifier, causing the air to cool down and lose some of its moisture, which exits the system as fresh liquid water. The dehumidifier also serves to preheat the saline water before entering the heater, which results in better energy efficiency than simple distillation.

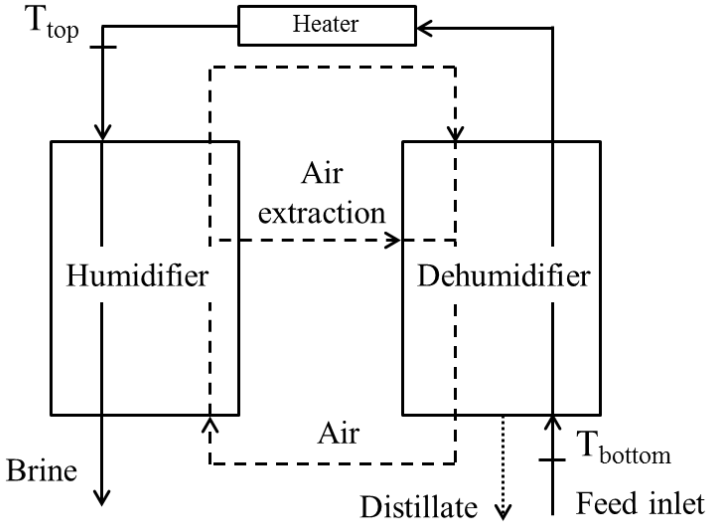

Figure 1: A schematic diagram of a humidification dehumidification (HDH) desalination system with a single air extraction/injection.

The major shortcoming of previous HDH systems has been their high energy consumption. This has spurred extensive research on improving the energy efficiency of these systems. Narayan et al. [5, 6] showed that the water-to-air mass flow rate ratio has a major effect on the energy efficiency of the system, and that a single value of the water-to-air mass flow rate ratio resulted in the highest energy efficiency. It was found that the condition for optimal performance was to set the modified heat capacity rate ratio (HCR_d) in the dehumidifier to unity, where HCR_d was defined in [7] as the ratio between the maximum change in the enthalpy rate of the cold stream to that of the hot stream:

$$\mathrm{HCR_d} = \frac{\Delta \dot{H}_{\mathrm{max,cold}}}{\Delta \dot{H}_{\mathrm{max,hot}}}$$

In addition, the specific heat of moist air varies greatly with temperature due to the latent heat of the water vapor, whereas the specific heat of water remains relatively constant. It is therefore beneficial to operate the system at a varied water-to-air mass flow rate ratio in order to keep the total heat capacity rates of the two streams as close as possible [8, 9, 10, 11, 12, 13, 14, 15]. This can be done by extracting an air stream from an intermediate location in the humidifier and injecting it at an intermediate location in the dehumidifier. In a recent study, it was found that the highest energy efficiency was achieved when the modified heat capacity rate ratio, HCR_d, was equal to 1 in each of the stages [16]:

$$\mathrm{HCR}_{\mathrm{d},1} = \mathrm{HCR}_{\mathrm{d},2} = 1$$

This paper studies the effect of feed salinity on the benefit that comes with operating the HDH system in two stages. The operation of a fixed-size HDH system under different feed salinities is simulated, and at each value of feed salinity the increase in efficiency and water production due to multi-staging is studied. In addition, the ability of HDH to treat a feed of varying salinity is studied by examining the flow rates that result in optimal performance at each feed salinity.

II. MODELING

The HDH system studied consists of a multi-tray bubble column dehumidifier and a packed-bed humidifier. This section briefly presents the models used, and the detailed descriptions of these models and their numerical solutions can be found in [17, 18] as well as in the Appendix.

2.1 Bubble Column Dehumidifier

Conventional dehumidifiers use a cold surface to condense water out of the air stream. However, the high concentration of air results in a very large resistance to water vapor mass transfer and necessitates a very large condensing surface. Narayan et al. [19] proposed the use of short bubble columns for the dehumidification side of HDH. Condensation in a bubble column occurs on the bubble-water interface, so the expensive metal surface required in previous dehumidifiers is replaced by a very large air-water interface.

In a bubble column dehumidifier, hot air bubbles travel through a column of fresh water and saline water travels through a coil that is submerged in the column. The air is cooled and dehumidified and the saline water is heated.

In this paper, the model developed by Tow and Lienhard [20] is used. This model uses a resistance network to model the heat and mass transfer between the air bubbles and the saline water. Tow and Lienhard assume perfect mixing in the column, which results in the air leaving the dehumidifier saturated at the temperature of the column. This means that the air-side resistance is negligible and there are only two resistances left: the outer resistance, R_{out}, between the coil and the column of fresh water, which is calculated using the correlation by Deckwer et al. [21], and the inner resistance, R_{in}, between the coil and the saline water, which is calculated using the correlations developed by Mori and Nakayama [22, 23]. Tow and Lienhard found that their model was in good agreement with experiments conducted at various conditions.

Although the bubble column may at first appear to be a counterflow heat and mass exchanger, it is effectively a parallel flow configuration. Both streams exchange heat with a column of fresh water which is well mixed and at a uniform temperature. This means that at best the two streams can exit at the same temperature, which is that of the column of fresh water. This results in a low effectiveness if only one column is used. The solution to this limitation is to stack up multiple trays in series to achieve high effectiveness. The equations above apply for a single tray, and modeling the multi-tray bubble column is a question of matching the boundary conditions between the successive trays. The numerical algorithm of the solution method can be found in [17, 24].

2.2 Packed-bed Humidifier

The packed-bed humidifier is modeled using the Poppe and Rögener cooling tower model [25]. This model is the most thorough model for cooling towers. It is widely used and has been experimentally verified [18]. The model was solved numerically using the fourth-order Runge-Kutta method, as described in great detail by Kloppers and Kröger [18, 26]. In this paper, the specifications provided by Brentwood Industries for their CF-1200MA packing (summarized in Table 1) are used to determine the performance of the packing. The equations summarizing the model as well as the solution algorithm can be found in the Appendix.

2.3 Complete System

In modeling a single-stage system, the packed-bed humidifier is coupled with the multi-tray bubble column and the air temperatures are matched between the two components, as shown in Fig. 1. The specifications of the system that are held constant are summarized in Table 1.

Table 1: Specifications of the system studied.

Operating conditions	
Top temperature	90 °C
Bottom temperature	25 °C
Feed mass flow rate	0.242 kg/s
Feed water salinity	0 - 200 ppt
Humidifier geometry	
Height, H	3 m
Cross-sectional area	0.05 m^2
Fill surface area	226 m^2 / m^3
Merkel number, Me	$0.967\left(\frac{\dot{m}_w}{\dot{m}_a}\right)^{-0.779} \times \left(3.28\,H\right)^{0.632}$
Minimum-maximum water loading	13.4-32 m^3 / hr - m^2
Dehumidifier geometry	
Pipe length per tray	2.5 m
Number of trays	30
Pipe outer / inner diameter	9.5 mm / 8.7 mm
Coil turn diameter	0.4 m

In order to model a two-stage system, the location of extraction/injection is varied, and the flow rates of dry air in the two stages are chosen such that the injected air stream is in equilibrium with the main stream in the dehumidifier at the point of injection. This condition means that there are only certain pairs of air flow rates that satisfy the requirement that no entropy is generated due to mixing at the point of injection. The location of extraction/injection and the flow rates of air are varied, and only the optimal conditions are presented in the following section. The numerical algorithms for the complete single-stage and two-stage systems are summarized in the Appendix, and are described in detail in [17].

2.4 Thermophysical Properties

The thermophysical properties of moist air and water vapor were evaluated using the ASHRAE Library of Humid Air Psychrometric & Transport Property (LibHuAirProp) which is based on ASHRAE RP-1485 [27].

The viscosity and conductivity of saline water were evaluated using the correlations presented by Sharqawy et al. [28]. The correlations for these variables are only verified up to a salinity of 160 ppt and had to be extrapolated to 200 ppt. However, these properties are only used in the calculation of the resistance of the liquid inside the coil in the bubble column dehumidifier, and the length of the pipe per tray is large enough such that this resistance is small and has minimal effect on the performance of the system.

In addition, the thermophysical properties of saline water were evaluated as those of aqueous NaCl based on the equations given in [29]. The air in the humidifier is in direct contact with the saline water, which lowers its water vapor pressure. In the equations describing the Poppe and Rögener model, the humidity ratio at saturation is evaluated using the reduced water vapor pressure.

2.5 Performance Parameters

The gained output ratio, GOR, is used to evaluate the energy efficiency of the system. It is defined as the ratio of the latent heat of vaporization of the product water to the heat input into the system:

$$\mathrm{GOR} = \frac{\dot{m}_{\mathrm{pw}} h_{\mathrm{fg}}}{\dot{Q}_{\mathrm{in}}}$$

In calculating GOR, the latent heat of vaporization, h_{fg}, was evaluated at the feed salinity and at 60 °C, which is representative of the operating range of temperatures.

The recovery ratio, RR, is the ratio of the mass flow rate of product water to that of the feed water:

$$\mathrm{RR} = \frac{\dot{m}_{\mathrm{pw}}}{\dot{m}_{\mathrm{feed}}}$$

In this paper, the feed flow rate, $\dot{m}_{\mathrm{feed}}$, is kept constant so RR is a direct measure of the water production in the system.

III. RESULTS

This section studies the effect of the feed salinity on the performance of a system of fixed-size, and on the increase in performance in going from single-stage to two-stage operation. In addition, this section explains why the use of a packed-bed humidifier decreases the effect of the decreasing vapor pressure on the system performance. The ability of HDH to handle varying feed salinity, up to 200 ppt, is also studied.

3.1 Effect of Salinity on the Gain from Multi-staging

As discussed in Section 1, operating a humidification dehumidification system in two stages with different mass flow rate ratios can help decrease the entropy generated and improve the energy efficiency of the system. This section evaluates the improvement in performance gained by going from a single-stage to a two-stage system while keeping the total system size constant.

At each value of feed salinity, the operating conditions that result in the best performance are found for single-stage and two-stage systems. The component dimensions and the operating conditions that are held constant are summarized in Table 1. For the single-stage case, the mass flow rate of dry air is varied, and the mass flow rate ratio that results in the best performance is that which also results in $HCR_d = 1$. To find the best performance that can be achieved by a two-stage system, the location of extraction/injection and the flow rates of dry air in the two stages are varied such that the injected stream is at the same temperature as the main stream in the dehumidifier at the location of injection. The combined sizes of the humidifiers and of the dehumidifiers are fixed. The operating conditions that result in the best performance for each salinity are those which result in $HCR_{d,1} = HCR_{d,2} = 1$, which is consistent with the results reported in [17] for seawater.

Figure 2 shows the highest GOR that can be achieved by optimized single-stage and two-stage systems of the same total size. It can be seen that the GOR of the single-stage system is not a strong function of the feed salinity. GOR for a feed salinity of 200 ppt is 11% lower than that at 0 ppt. This result is comparable to the findings of Thiel et al. [30] who report that a GOR drop of around 17-27% by going from a feed salinity of 0 to 260 ppt by using a fixed temperature pinch. It is expected that the drop will further increase as salinity is increased to 260 ppt.

The performance of the two-stage system drops with increasing salinity. However, as shown in Fig. 3, the gain in GOR as a result of multi-staging is still sizeable. The increase in GOR drops from around 60% at 0 ppt to around 40% at 200 ppt. It is worth noting that these numbers are specific to the system simulated in this paper, which is large enough to result in high component effectiveness ($\varepsilon_d = 98\%$, $\varepsilon_h = 92\%$) when operated as a single stage. As the system size decreases, the improvement in performance would decrease because the portion of entropy generation saved by better balancing becomes smaller compared to the total entropy generated in the system.

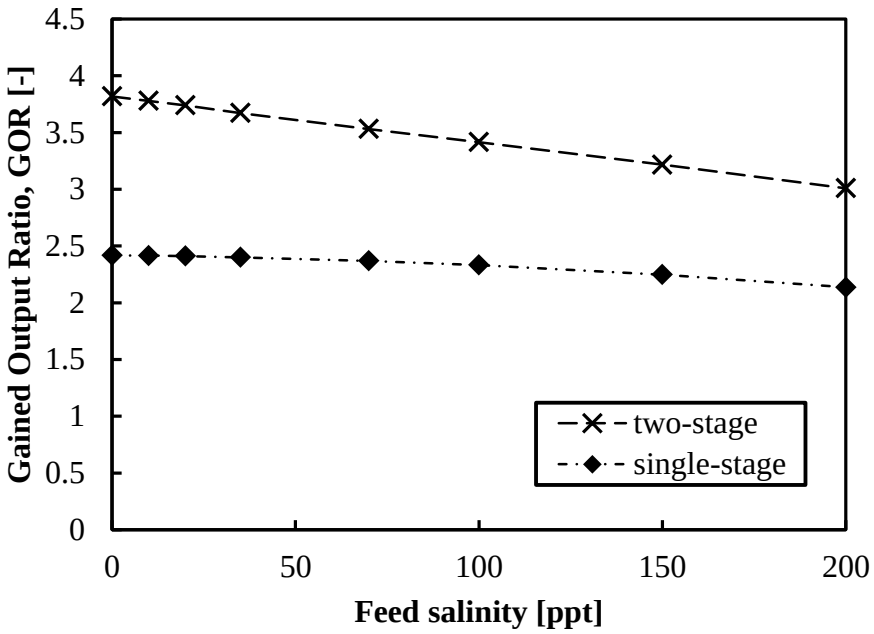

Figure 2: Variation of GOR with feed salinity for a single-stage system and a two-stage system of the same size.

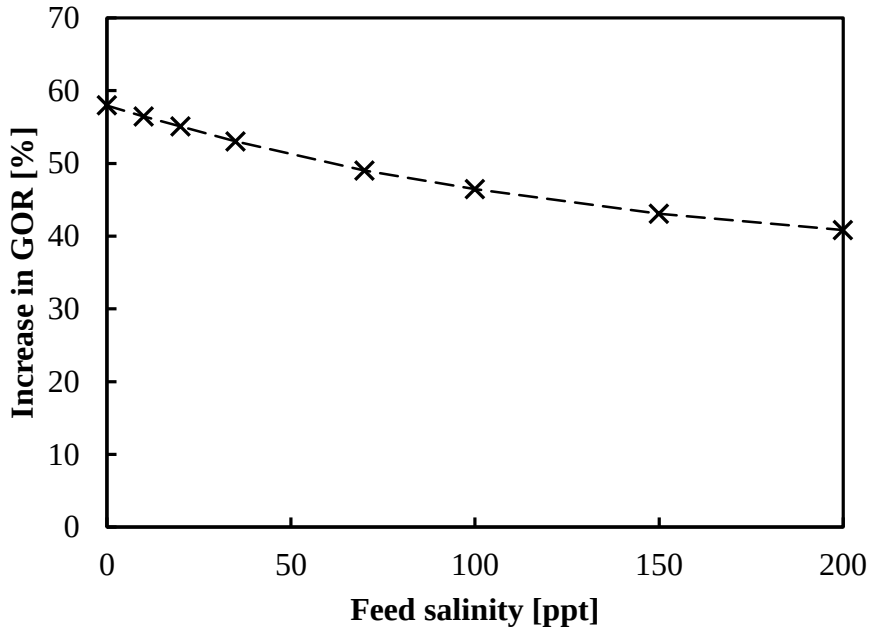

Figure 3: Variation of the improvement in GOR with feed salinity when going from a single-stage system to a two-stage system of the same size.

Figure 4 shows the effect of a single air extraction on the recovery ratio. It can be seen that the recovery ratio is not a strong function of salinity. It remains constant at around 7.5% for the single-stage system, and decreases form 8.3% to 7.9% for the two-stage system when the salinity is increased from 0 to 200 ppt. As was shown in previous studies [11, 14, 24], the effect of multi-staging has a much higher impact on the energy efficiency than on the water recovery.

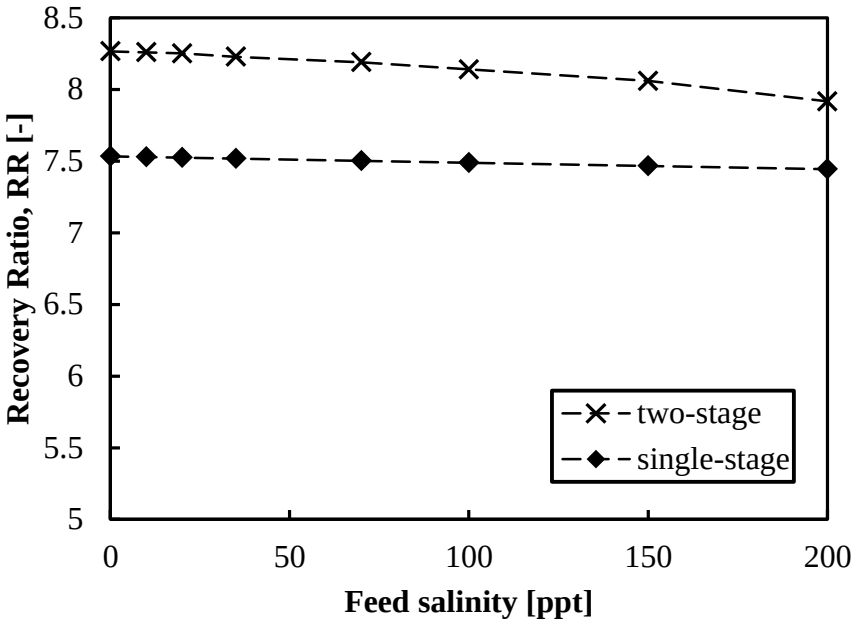

Figure 4: Variation of the recovery ratio, RR, with the feed salinity for a single-stage system and a two-stage system of the same size.

3.2 Reduced Effect of Salinity on Vapor Pressure

As explained in Section 2, salinity affects many properties of water, thus affecting the performance of an HDH system. The most important effect of salinity is that it decreases the vapor pressure of water in the humidifier where the air is in direct contact with saline water. This decrease in vapor pressure decreases the humidity ratio that saturated air can achieve. It is therefore expected that the amount of water carried by the air decreases with increasing salinity. However, in the case of a packed-bed humidifier, the air can reach supersaturation, with the water content above saturation condensing and remaining in the air stream in the form of fine mist. This phenomenon can be seen above the cooling towers used in power plants where the high content of mist gives the discharged air stream its white color.

According to Kloppers and Kröger [26], once the air in the humidifier reaches supersaturation it will remain supersaturated until it exits the humidifier. This means that the water that can be carried by the air stream is not limited by the saturation curve, and that the additional water content will only condense when it enters the dehumidifier.

Figure 5 shows the temperature profile of the different streams under optimal operating conditions at a feed salinity of 100 ppt. As proposed by McGovern et al. [10], the specific enthalpy is expressed per unit mass of dry air so that all the curves can be superposed on the same graph. It can be seen that the air in

the humidifier does not follow the saturation curve corresponding to 100 ppt and that it is in fact supersaturated. It follows a path that is close to that followed by the air in the dehumidifier, which is saturated and in contact with *pure* water in the bubble column. The air exits the humidifier with some water content in the form of mist, which is condensed as soon as it enters the dehumidifier. This means that the lower vapor pressure does not limit the water content that can be carried by the air, and its only effect is that it decreases the driving force to mass transfer in the humidifier, reducing the performance slightly.

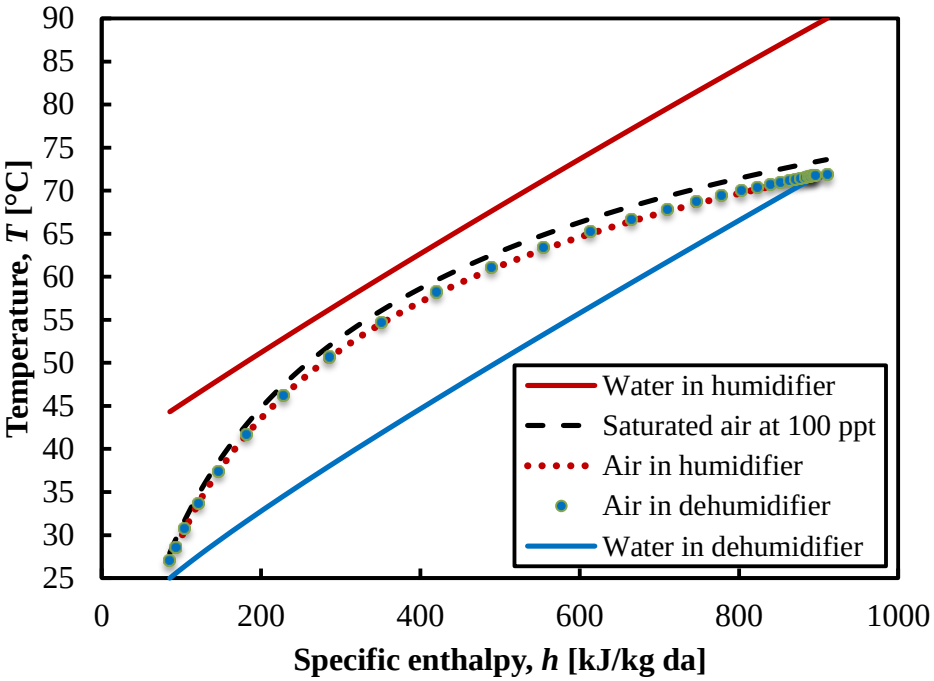

Figure 5: Temperature-enthalpy profile of a single-stage system with a feed salinity of 100 ppt.

3.3 Ability of HDH to Respond to Varying Salinity

This section examines the ability of HDH to respond to varying feed salinity, which is relevant to treating water from hydraulically fractured wells. As the age of the well increases, so does the salinity of the produced water [31].

Figure 6 shows that the optimal water-to-air mass flow rate ratio, MR, for this system goes from 4.2 to 4.8 when the salinity goes from 0 to 200 ppt, where

$$\mathrm{MR} = \frac{\dot{m}_{\mathrm{w}}}{\dot{m}_{\mathrm{da}}}$$

Figure 7 shows the variation of the GOR of two systems with feed salinity. The first system adjusts its mass flow rate ratio to maintain optimal energy efficiency regardless of the feed salinity. It operates under the values of the mass flow rate ratio shown in Fig. 6. The second system always operates at the mass flow rate ratio that yields optimal performance only at 100 ppt (MR = 4.5). The two systems yield a very similar performance, and it is clear that there is very little loss in GOR by not operating under a varying mass flow rate ratio. The effect of varying feed salinity on the performance of the system is

much smaller than that of the top and bottom temperatures, as reported in [24]. This makes HDH suitable for applications where the feed salinity varies greatly such as treating produced water from shale wells.

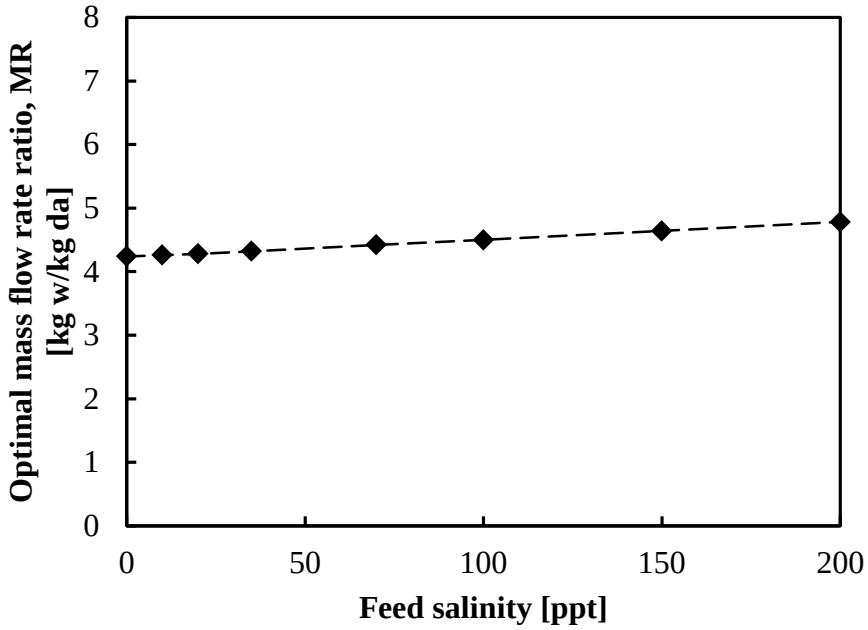

Figure 6: Variation of the optimal water-to-air mass flow rate ratio, MR, with the feed salinity.

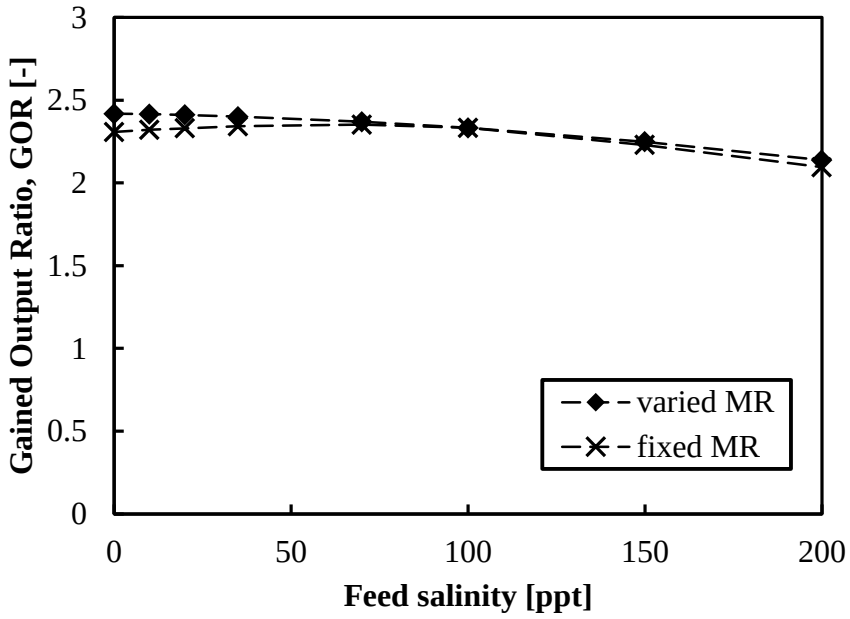

Figure 7: Effect of salinity on the performance of (a) a system with an optimal mass flow rate ratio, and (b) a system with its mass flow rate ratio fixed at the optimal for 100 ppt.

IV. CONCLUSIONS

In this paper the operation of a humidification dehumidification system under varying feed salinity is modeled. The following conclusions are reached:

- It is beneficial to implement a variation of the mass flow rate ratio through extraction/injection even at high salinity.
- The negative effects of rising salinity on GOR are reduced because air in the humidifier can reach a supersaturated state that is not limited by the water content at saturation.
- HDH is suitable for operation under varying feed salinity because the optimal mass flow rate ratio is not a strong function of feed salinity.

V. ACKNOWLEDGEMENTS

We would like to thank the King Fahd University of Petroleum and Minerals for funding the research reported in this paper through the Center for Clean Water and Clean Energy at MIT and KFUPM (Project #R4-CW-08). In addition, we would like to thank Gregory Thiel for providing the MATLAB implementation of the aqueous sodium chloride properties.

VI. APPENDIX

6.1 Bubble Column Dehumidifier Model

The bubble column dehumidifier is modeled using Tow and Lienhard's model [20]. The equations used in the model are the following:

A water mass balance:

$$\dot{m}_{\mathrm{cond,out}} = \dot{m}_{\mathrm{cond,in}} + \dot{m}_{\mathrm{da}}(\omega_{\mathrm{in}} - \omega_{\mathrm{out}})$$

where $\dot{m}_{\mathrm{cond,out}}$ is the mass flow rate of the condensate leaving the bubble column, and $\dot{m}_{\mathrm{da}}$ is that of the dry air. ω is the humidity ratio.

An energy balance:

$$\dot{m}_{\mathrm{da}}\left(h_{\mathrm{a,in}} - h_{\mathrm{a,out}}\right) + \dot{m}_{\mathrm{cond,in}}h_{\mathrm{cond,in}} - \dot{m}_{\mathrm{cond,out}}h_{\mathrm{cond,out}} = \dot{m}_{\mathrm{w}}\left(h_{\mathrm{w,out}} - h_{\mathrm{w,in}}\right) = \dot{Q}$$

where h_{a} is the enthalpy of the moist air, and h_{w} is that of the saline water.

The heat transferred to the water stream can be calculated as follows:

$$\dot{Q} = \frac{\Delta T_{\mathrm{lm}}}{R_{\mathrm{in}} + R_{\mathrm{out}}}$$

where the logarithmic mean temperature difference is defined as:

$$\Delta T_{\mathrm{lm}} = \frac{T_{\mathrm{w,out}} - T_{\mathrm{w,in}}}{\ln\left(\frac{T_{\mathrm{col}} - T_{\mathrm{w,in}}}{T_{\mathrm{col}} - T_{\mathrm{w,out}}}\right)}$$

and T_{col} is the column temperature.

6.2 Packed-bed Humidifier Model

The equations used in the model presented by Kloppers and Kröger [18, 26] are summarized as follows:

The Lewis factor according to Bosnjakovic [32]:

$$Le_{\mathrm{f}} = 0.865^{0.667}\left(\frac{\omega_{\mathrm{sw}} + 0.622}{\omega_{\mathrm{sa}} + 0.622} - 1\right)\left[\ln\left(\frac{\omega_{\mathrm{sw}} + 0.622}{\omega_{\mathrm{sa}} + 0.622}\right)\right]^{-1}$$

The governing equations for supersaturation:

$$\mathrm{X} = h_{\mathrm{a,sw}} - h_{\mathrm{a,ss}} + (Le_{\mathrm{f}} - 1)\left[h_{\mathrm{a,sw}} - h_{\mathrm{a,ss}} - (\omega_{\mathrm{sw}} - \omega_{\mathrm{sa}})h_{\mathrm{v}} - (\omega_{\mathrm{sa}} - \omega)c_{\mathrm{p,w}}T_{\mathrm{w}}\right] - (\omega_{\mathrm{sw}} - \omega)c_{\mathrm{p,w}}T_{\mathrm{w}}$$

$$\frac{dh_{\mathrm{a}}}{dT_{\mathrm{w}}} = \frac{\dot{m}_{\mathrm{w}}c_{\mathrm{p,w}}}{\dot{m}_{\mathrm{a}}}\left(1 + \frac{(\omega_{\mathrm{sw}} - \omega_{\mathrm{sa}})c_{\mathrm{p,w}}T_{\mathrm{w}}}{\mathrm{X}}\right)$$

$$\frac{d\omega}{dT_{\mathrm{w}}} = \frac{\dot{m}_{\mathrm{w}}c_{\mathrm{p,w}}}{\dot{m}_{\mathrm{a}}}\left(\frac{\omega_{\mathrm{sw}} - \omega_{\mathrm{sa}}}{\mathrm{X}}\right)$$

$$\frac{dMe}{dT_{\mathrm{w}}} = \frac{c_{\mathrm{p,w}}}{\mathrm{X}}$$

The subscript ‘sa’ means that the property is evaluated at saturation at the air temperature, and the subscript ‘ss’ denotes supersaturation.

The solution algorithm is presented in Fig. 8 below.

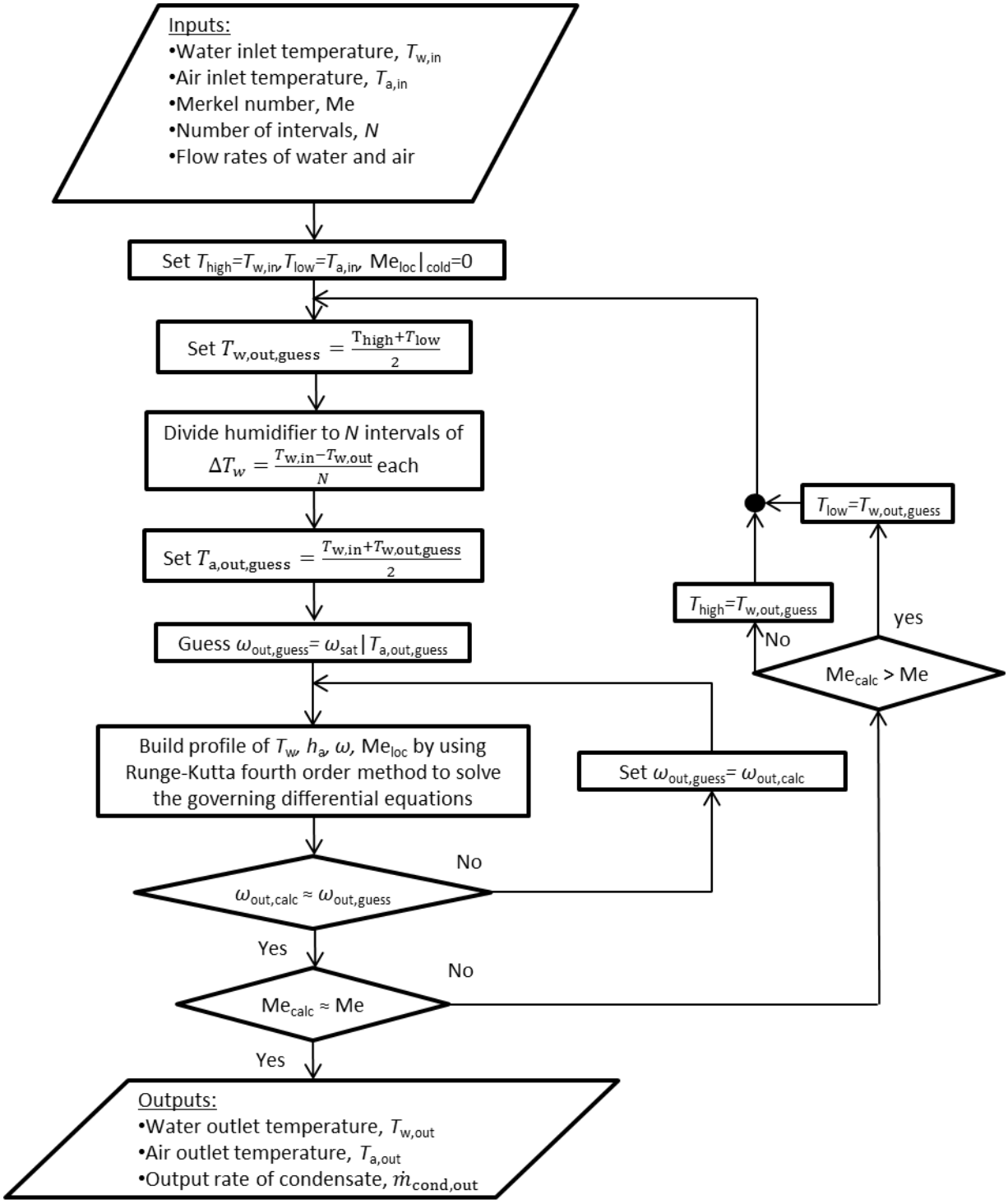

Figure 8: Solution algorithm for the humidifier model [17].

6.3 Single-stage System Solution Algorithm

The solution algorithm for the single-stage system consists of simply coupling a humidifier and a dehumidifier. Given that the top and bottom air temperatures are not known, the dehumidifier and the humidifier cannot be simulated independently. The bottom air temperature is guessed, the humidifier is then simulated and the top air temperature is calculated. The dehumidifier is then simulated and the lower air temperature is updated. The procedure is repeated until the error on the bottom air temperature is small enough.

6.4 Two-stage System Solution Algorithm

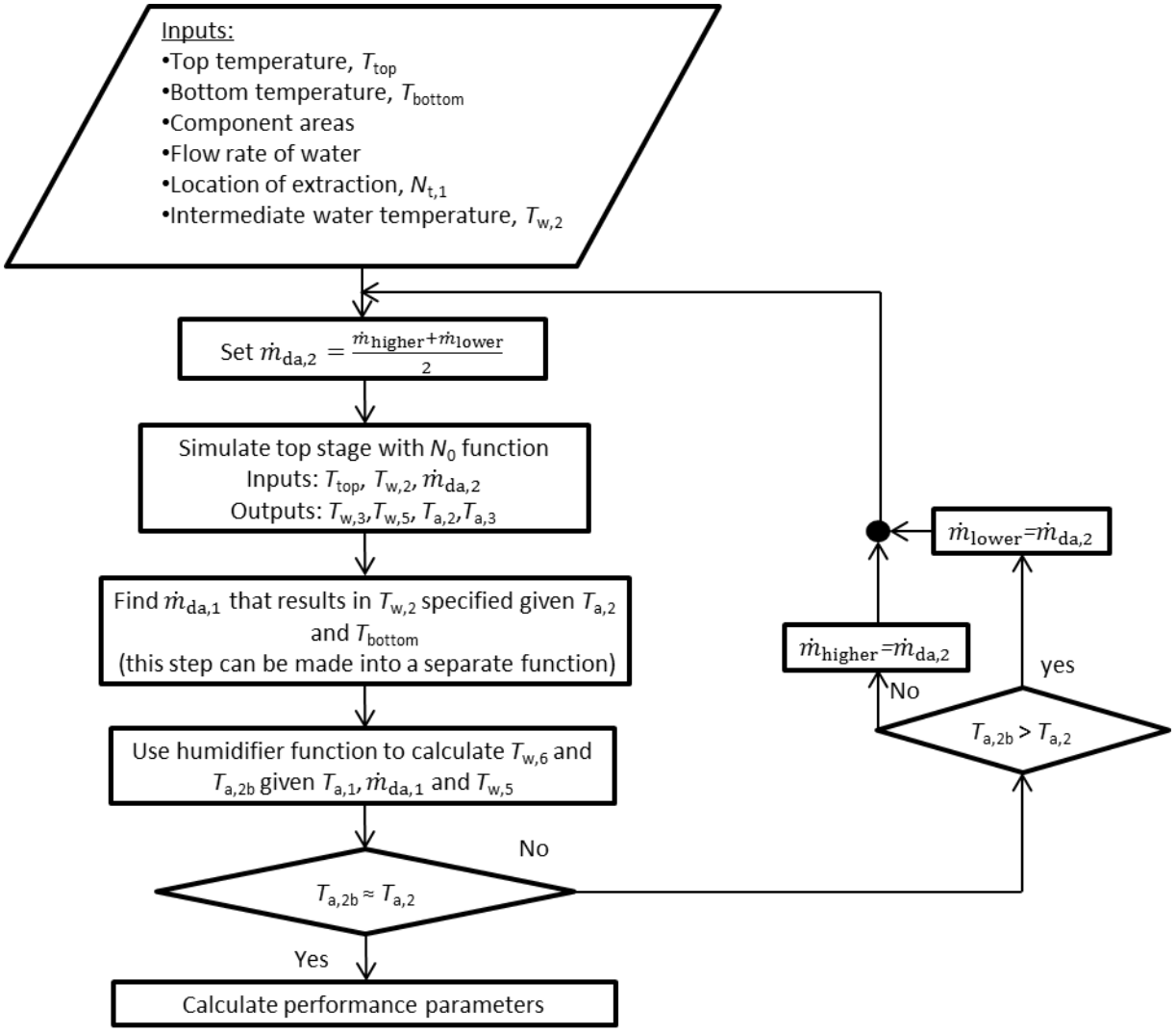

Figure 9: Solution algorithm for the two-stage system [17]**.**

VII. REFERENCES

[1] G. P. Narayan and J. H. Lienhard V, "Thermal Design of Humidification Dehumidification Systems for Affordable Small-scale Desalination," *IDA Journal,* vol. 4, pp. 24-34, 2012.

[2] G. P. Narayan and J. H. Lienhard V, "Humidification-dehumidification desalination," in *Desalination: Water from Water,* Salem, MA, Wiley-Scrivener, 2014.

[3] P. G. Narayan, M. H. Sharqawy, E. K. Summers, J. H. Lienhard V, S. M. Zubair and M. A. Antar, "The potential of solar-driven humidification-dehumidification desalination for small-scale decentralized water production," *Renewable and Sustainable Energy Reviews,* vol. 14, pp. 1187-1201, 2010.

[4] T. Pankratz, "HDH tackles brine disposal challenge," *Water desalination report,* pp. 2-3, 6 May 2014.

[5] G. P. Narayan, J. H. Lienhard V and S. M. Zubair, "Entropy generation minimization of combined heat and mass transfer," *International Journal of Thermal Sciences,* vol. 49, pp. 2057-66, 2010.

[6] G. P. Narayan, M. H. Sharqawy, J. H. Lienhard V and S. M. Zubair, "Thermodynamic analysis of humidification-dehumidification desalination cycles," *Desalination and Water Treatment,* vol. 16, pp. 339-353, 2010.

[7] G. P. Narayan, K. H. Mistry, M. H. Sharqawy, S. M. Zubair and J. H. Lienhard V, "Energy Effectiveness of Simultaneous Heat and Mass Exchange Devices," *Frontiers in Heat and Mass Transfer,* vol. 1, pp. 1-13, 2010.

[8] H. Muller-Holst, "Solar thermal desalination using the Multiple Effect Humidification (MEH) method in Solar Desalination for the 21st Century," in *NATO Security through Science Series,* Springer, Dordrecht, 2007, pp. 215-25.

[9] M. Zamen, S. M. Soufari and M. Amidpour, "Improvement of Solar Humdification-Dehumidification Desalination Using Multi-Stage Process," *Chemical Engineering Transactions,* vol. 25, pp. 1091-1096, 2011.

[10] R. K. McGovern, G. P. Thiel, G. P. Narayan, S. M. Zubair and J. H. Lienhard V, "Performance Limits of zero and single extraction Humidification Dehumidification Desalination Systems," *Applied Energy,* vol. 102, pp. 1081-1090, 2013.

[11] G. P. Narayan, K. M. Chehayeb, R. K. McGovern, G. P. Thiel, S. M. Zubair and J. H. Lienhard V, "Thermodynamic balancing of the humidification dehumidification desalination system by mass extraction and injection," *International Journal of Heat and Mass Transfer,* vol. 57, no. 2, pp. 756-770, 2013.

[12] J. A. Miller and J. H. Lienhard V, "Impact of extraction on a humidification dehumidification desalination system," *Desalination,* vol. 313, pp. 87-96, 2013.

[13] G. P. Thiel, J. A. Miller, S. M. Zubair and J. H. Lienhard V, "Effect of mass extractions and injections on the performance of a fixed-size humidification–dehumidification desalination system," *Desalination,* vol. 314, pp. 50-58, 2013.

[14] K. M. Chehayeb, G. P. Narayan, S. M. Zubair and J. H. Lienhard V, "Use of multiple extractions and injections to thermodynamically balance the humidification dehumidification desalination system," *International Journal of Heat and Mass Transfer,* vol. 68, pp. 422-434, 2014.

[15] G. P. Narayan, M. G. St. John, S. M. Zubair and J. H. Lienhard V, "Thermal design of the humidification dehumidification desalination system: An experimental investigation," *International Journal of Heat and Mass Transfer,* vol. 58, pp. 740-748, 2013.

[16] K. M. Chehayeb, G. P. Narayan, S. M. Zubair and J. H. Lienhard V, "Thermodynamic balancing of a fixed-size two-stage humidification dehumidification desalination system," *Desalination,* vol. 369, pp. 125-139, 2015.

[17] K. M. Chehayeb, Numerical fixed-effectiveness and fixed-area models of the humidification dehumidification desalination system with air extractions and injections, Master's thesis, Cambridge: Massachusetts Institute of Technology, 2014.

[18] J. C. Kloppers, A critical evaluation and refinement of the performance prediction of wet-cooling towers, PhD thesis, Stellenbosch: University of Stellenbosch, 2003.

[19] G. P. Narayan, M. H. Sharqawy, S. Lam, S. K. Das and J. H. Lienhard V, "Bubble columns for condensation at high concentrations of noncondensable gas: Heat-transfer model and experiments," *AIChE Journal,* vol. 59, pp. 1780-1790, 2013.

[20] E. W. Tow and J. H. Lienhard V, "Experiments and Modeling of Bubble Column Dehumidifier Performance," *International Journal of Thermal Sciences,* vol. 80, pp. 65-75, 2014.

[21] W. D. Deckwer, "On the mechanism of heat transfer in bubble column reactors," *Chemical Engineering Science,* vol. 35, pp. 1341-1346, 1980.

[22] Y. Mori and W. Nakayama, "Study on forced convective heat transfer in curved pipes: (1st report, laminar region)," *International Journal of Heat and Mass Transfer,* vol. 8, pp. 67-82, 1965.

[23] Y. Mori and W. Nakayama, "Study of forced convective heat transfer in curved pipes (2nd report, turbulent region)," *International Journal of Heat and Mass Transfer,* vol. 10, pp. 37-59, 1967.

[24] K. M. Chehayeb, F. K. Cheaib and J. H. Lienhard V, "A numerical solution algorithm for a heat and mass transfer model of a desalination systems based on packed-bed humidification and bubble column dehumidification," in *Proc. 15th Intl. Heat Transfer Conference, IHTC-15*, Kyoto, Japan, 2014.

[25] M. Poppe and H. Rögener, "Berechnung von rückkühlwerken," *VDI-Wärmeatlas,* vol. 111, pp. 1-15, 1991.

[26] J. C. Kloppers and D. G. Kroger, "A critical investigation into the heat and mass transfer analysis of counterflow wet-cooling towers," *International Journal of Heat and Mass Transfer,* vol. 48, pp. 765-777, 2005.

[27] S. Herrmann, H. J. Kretzschmar and D. P. Gatley, "Thermodynamic properties of real moist air, dry air, steam, water, and ice (rp-1485)," *HVAC&R Research,* vol. 15, p. 961–986, 2009.

[28] M. H. Sharqawy, J. H. Lienhard V and S. M. Zubair, "Thermophysical properties of seawater: A review of existing correlations and data," *Desalination and water treatment,* vol. 16, pp. 354-380, 2010.

[29] K. S. Pitzer, J. C. Peiper and R. H. Busey, "Thermodynamic properties of aqueous sodium chloride solutions," *Journal of Physical and Chemical Reference Data,* vol. 13, pp. 1-102, 1984.

[30] G. P. Thiel, E. T. Tow, L. D. Banchik, H. W. Chung and J. H. Lienhard V, "Energy consumption in desalinating produced water from shale oil and gas extraction," *Desalination,* accepted 2015.

[31] G. P. Thiel, S. M. Zubair and J. H. Lienhard V, "An analysis of likely scalants in the treatment of produced water from Nova Scotia," *Heat Transfer Engineering,* vol. 36, pp. 652-662, 2015.

[32] F. Bosnjakovic, Technical thermodynamics, Holt, Rinehart and Winston, 1965.